

# Doppler-Radar-Based Short-Range Acquisitions of Time-Frequency Signatures from an Industrial-Type Wind Turbine

José-María Muñoz-Ferreras<sup>#</sup>, Zhengyu Peng<sup>\*</sup>, Yao Tang<sup>\*</sup>, Roberto Gómez-García<sup>#</sup>, Changzhi Li<sup>\*</sup>

<sup>#</sup>Dept. Signal Theory & Commun., Univ. Alcalá, Alcalá de Henares 28871, Spain

<sup>\*</sup>Dept. Electrical & Computer Engineer., Texas Tech University, Lubbock, TX 79409, USA

**Abstract**—Non-contact radar-based monitoring of large mechanical constructions is currently gaining much attention from the RF/microwave community. In particular, Doppler radars can be coherently exploited to extract spectrograms—i.e., time-Doppler maps—of industrial-type wind turbines. This work conducts short-range experiments corresponding to a 50-m-height Vestas wind turbine illuminated by two custom-designed quadrature radar prototypes operating at 5.8 and 24 GHz, respectively. It is observed that the obtained experimental radar signatures—that are shaped by flashes and quasi-sinusoidal halos—exhibit distinct characteristics depending on the acquisition geometry and the operation frequency of the radar sensor. These features might lead in the future to a radar-based non-contact monitoring solution of the structural health of industrial-type wind turbines.

**Index Terms**—Doppler radars, structural health monitoring (SHM), wind turbines, wireless sensors.

## I. INTRODUCTION

Radars are non-contact wireless devices that can retrieve useful information from surrounding targets. In particular, coherent radars can be sensitive enough to detect small motions, such as vital signs or vibrations in huge mechanical constructions, such as buildings or bridges [1], [2]. In the specific case of Doppler radars, they can obtain finely-detailed time-Doppler maps (i.e., spectrograms) that could be exploited for subsequent signal-processing tasks [3].

As an example of the latter, untypical vibrations of a monitored construction might leave a detectable signature in the spectrograms. For industrial-type wind turbines, this means that it might be possible to infer some defects or malfunctionings (e.g., unbalanced loads, cracks of the blades, tip damages, or an excessive bending of the blades) from the corresponding time-Doppler maps [3], [4]. This could pave the way for the potential radar-based monitoring of the structural health of this kind of wind turbines.

Coherent radar signatures of wind turbines consist of the well-known flashes and tip halos [5], [6]. Some works have been carried out in the past with regard to short-range acquisitions from small models [5] and long-range campaigns for big turbines [6]. This paper complements these studies by reporting short-range experiments for an industrial-type 50-m-height wind turbine Vestas V47 from the American Wind Power Center, Lubbock, TX, USA [3]. Two custom-designed quadrature Doppler radars operating

TABLE I  
PARAMETERS OF THE DOPPLER RADAR PROTOTYPES

	Prototype I	Prototype II
Center frequency ( $f_c$ )	5.8 GHz	24 GHz
Average transmitted power	8 dBm	8 dBm
Antenna directivity	11.8 dBi	19.8 dBi
Sampling frequency ( $f_s$ )	44.1 kHz	44.1 kHz

at 5.8 and 24 GHz have been developed to perform the wind-turbine illumination [3].

This paper supplements with real experiments the studies previously reported by the authors in [4] and [7]. In comparison with [3], more experiments and tests for different geometries are accomplished. Also, the differences observed in the spectrograms when using distinct operation frequencies are emphasized. In particular, the experimental data corresponding to the 24-GHz radar prototype indicate the presence of unconventional quasi-sinusoidal histories, which might be attributed to scattering discontinuities (e.g., small cracks). A close-up analysis of the Vestas-V47 blades (e.g., with a crane or with a drone) is left as future work. If confirmed, radar-based structural health monitoring (SHM) of industrial-type wind turbines might be feasible.

## II. DESCRIPTION OF THE RADAR PROTOTYPES

The two radar prototypes were designed and implemented by the authors [3]. Their main features are listed in Table I. These radar systems can work in three operation modes: the Doppler mode, the frequency-modulated continuous-wave (FMCW) mode, and the hybrid mode which multiplexes in time the two previous ones. Here, only the Doppler mode is exploited. Moreover, both systems use a two-channel audio card to acquire the baseband in-phase and quadrature ( $I/Q$ ) signals. These  $I/Q$  components were obtained in two different ways: after a mixer-based demodulation for the 5.8-GHz radar and after a six-port-based downconversion for the 24-GHz prototype [3].

## III. ACQUISITION SCENARIO

Fig. 1 shows a bird's eye view for the acquisition scenario in the American Wind Power Center, Lubbock, TX, USA. The illuminated industrial-type 660-kW Vestas V47 wind turbine has a blade length of  $L_b = 23.5$  m and a tower height of  $H_t = 50$  m. Two positions for

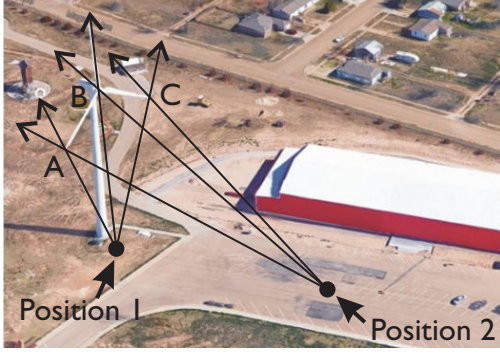


Fig. 1. Acquisition scenario with indication of positions 1 and 2, and radar pointings A, B, and C. Source: Google Earth<sup>TM</sup>.

the radar systems were considered: on the ground under the wind-turbine rotor (position 1), and far from the wind turbine with an aspect angle of about  $90^\circ$  (position 2). The blades were rotating clockwise (Fig. 1). Furthermore, the two radar sensors were manually pointed at directions A, B, and C, which correspond to the receding blades, the rotor hub, and the approaching blades, respectively.

#### IV. EXPERIMENTAL RESULTS

In this section, the experimental results obtained for the Vestas V47 wind turbine illuminated with the developed 5.8- and 24-GHz radar systems are reported and discussed.

##### A. Radar Prototype I

The 5.8-GHz radar sensor has a lower directivity. This means that the wind-turbine rotor is fully contained within the antenna beam regardless of the pointing direction. Fig. 2 shows the spectrogram obtained for positions 1 and 2.

As can be seen, the spectrograms are shaped by energetic flashes and quasi-sinusoidal halos. Fig. 2(a) shows flashes with a maximum Doppler frequency of  $f_{Dop,max} \approx 2750$  Hz. This can be justified after estimating the rotation period from the time appearance of the flashes ( $T \approx 2.1$  s) that leads to a theoretical value of  $f_{Dop,max} = 4\pi L_b f_c / (cT) \approx 2718.7$  Hz. The tilting of the flashes is a short-range effect [3], [7]. In relation to Fig. 2(b), the maximum Doppler is reduced due to the geometry. Besides, the curvature of the flashes for position 2 is manifest when compared to the spectrogram for position 1 [3], [7]. Note that theoretical justifications and simulations corroborate these features [3], [7].

##### B. Radar Prototype II

The antenna directivity for the 24-GHz radar prototype is higher (see Table I). This means that the blades are not completely contained within the radar beam. Fig. 3 shows the spectrograms for positions 1 and 2 when the pointing direction is A (see Fig. 1). As observed in Fig. 3(a), the negative-Doppler flashes corresponding to the receding blades (direction A) are noticeable. The maximum Doppler frequency is approximately  $f_{Dop,max} \approx 11.4$  kHz, which

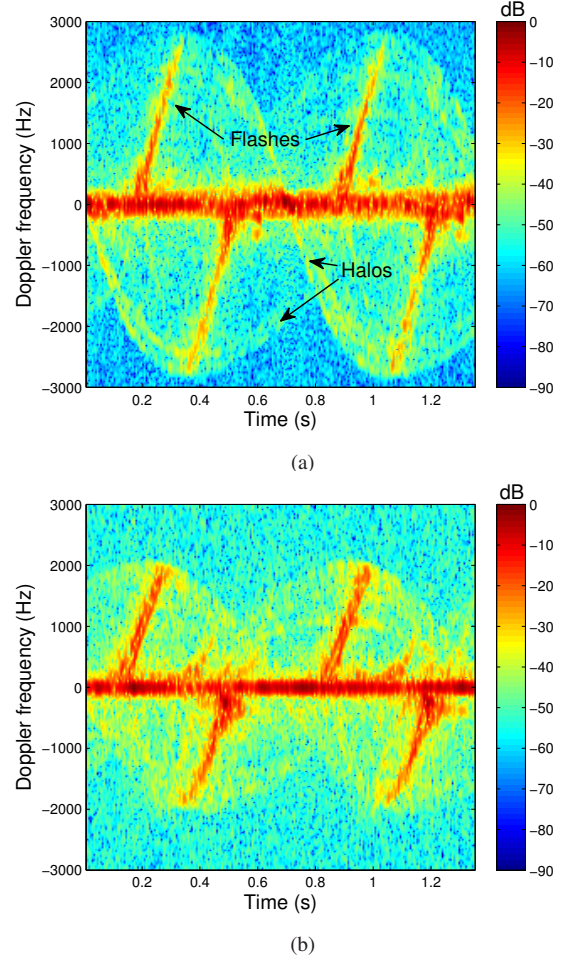


Fig. 2. Spectrograms for the wind turbine illuminated by the 5.8-GHz radar prototype. Spectrogram parameters: Hamming window of 512 samples and Fast Fourier Transform (FFT) of 4096 points. (a) Position 1. (b) Position 2.

is consistent with the rotation period estimated to be  $T \approx 2.1$  s. Since the approaching blades are not fully illuminated in this case, the positive-Doppler flashes are not completely identifiable. In addition, the flashes in Fig. 3(b) exhibit more curvature and are wider than the ones depicted in Fig. 3(a), like in the results in Section IV-A. This phenomenon is attributed to the geometry and the different cross-section views for positions 1 and 2 [3], [7].

Interestingly, Fig. 3(a) shows some unconventional quasi-sinusoidal histories, observed for this higher-resolution 24-GHz prototype. Further work will include a close-up view of the blades to confirm if these scattering anomalies might be attributed to defects in their surface. On the other hand, the mirrored flashes—which can be also verified through simulation—are attributed to  $I/Q$  mismatches in the receiver chain of the 24-GHz radar device—specifically, in its mixing six-port circuit [3].

When pointing at the rotor hub (direction B in Fig. 1), the tips of the blades are not contained within the radar beam. The experimental results for this situation are



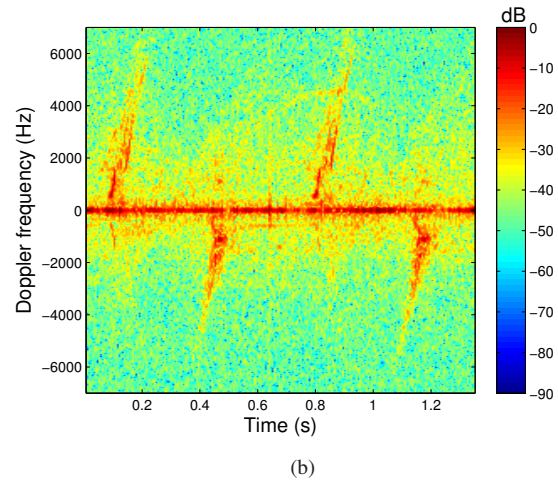
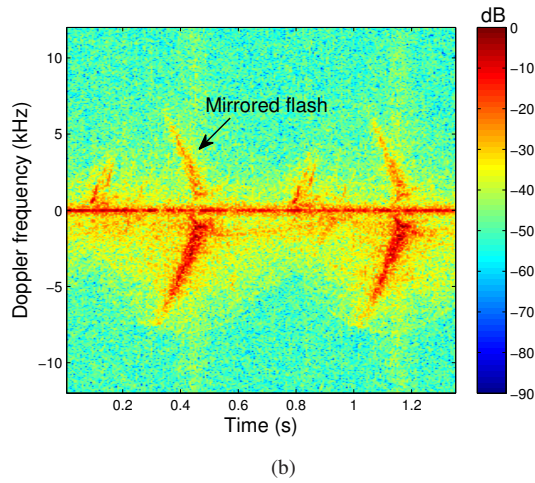
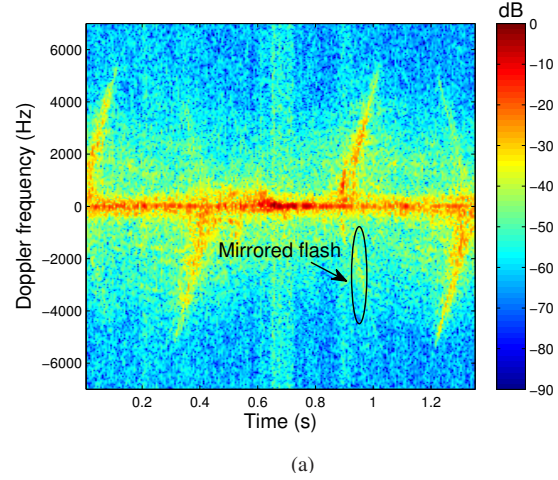
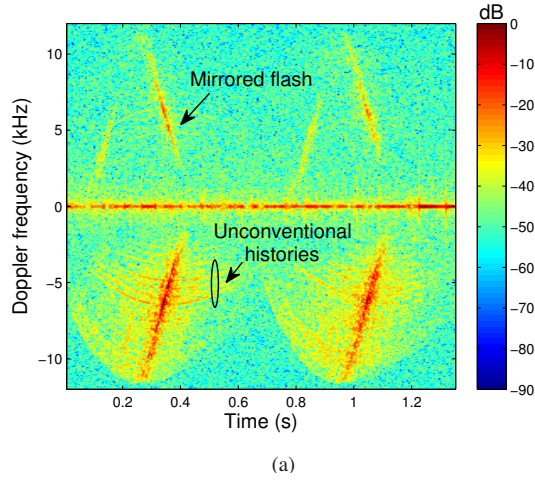


Fig. 3. Spectrograms for the wind turbine illuminated by the 24-GHz radar prototype at the pointing direction A. Spectrogram parameters: Hamming window of 512 samples and FFT of 4096 points. (a) Position 1. (b) Position 2.

Fig. 4. Spectrograms for the wind turbine illuminated by the 24-GHz radar prototype at the pointing direction B. Spectrogram parameters: Hamming window of 512 samples and FFT of 4096 points. (a) Position 1. (b) Position 2.

detailed in Fig. 4. Note that the Doppler excursion for the flashes is not complete. Nevertheless, the results are analogous to the ones reported in Fig. 3. The experimental results for the pointing C—not included here for room reasons—are also analogous to the ones shown in Fig. 3.

## V. CONCLUSION

This work has presented short-range remote-sensing experiments for an industrial-type 50-m-height wind turbine illuminated by two custom-designed Doppler radar prototypes operating at 5.8 and 24 GHz, respectively. The referred spectrograms have been shown for different acquisition geometries. The features of the time-Doppler maps might be exploited in the future for structural health monitoring (SHM) of this type of wind turbines.

## REFERENCES

- [1] C. Li, V. M. Lubecke, O. Boric-Lubecke, and J. Lin, "A review on recent advances in Doppler radar sensors for noncontact healthcare monitoring," *IEEE Trans. Microw. Theory Techn.*, vol. 61, no. 5, pp. 2046–2060, May 2013.
- [2] C. Gu, G. Wang, J. A. Rice, and C. Li, "Interferometric radar sensor with active transponders for signal boosting and clutter rejection in structural health monitoring," in *Proc. IEEE MTT-S Int. Microw. Symp. Dig.*, Montreal, QC, Canada, Jun. 2012, pp. 1–3.
- [3] J. M. Muñoz-Ferreras, Z. Peng, Y. Tang, R. Gómez-García, D. Liang, and C. Li, "Short-range Doppler-radar signatures from industrial wind turbines: theory, simulations, and measurements," *IEEE Trans. Instrum. Meas.*, Early Access, pp. 1–12, Jun. 2016.
- [4] T. Nikoubin, J. M. Muñoz-Ferreras, R. Gómez-García, D. Liang, and C. Li, "Structural health monitoring of wind turbines using a low-cost portable K-band radar: An ab-initio field investigation," in *Proc. IEEE Topical Conf. Wireless Sensors Sensor Netw. (WiSNet)*, San Diego, CA, USA, Jan. 2015, pp. 69–71.
- [5] A. Naqvi, S.-T. Yang, and H. Ling, "Investigation of Doppler features from wind turbine scattering," *IEEE Antennas Wireless Propag. Lett.*, vol. 9, pp. 485–488, 2010.
- [6] A. Buterbaugh *et al.*, "Dynamic radar cross section and radar Doppler measurements of commercial general electric windmill power turbines, part 2—Predicted and measured Doppler signatures," in *Proc. Antenna Meas. Techn. Assoc. (AMTA) Symp.*, St. Louis, MO, USA, Nov. 2007, pp. 1–6.
- [7] J. M. Muñoz-Ferreras, Z. Peng, Y. Tang, R. Gómez-García, D. Liang, and C. Li, "A step forward towards radar sensor networks for structural health monitoring of wind turbines," in *Proc. IEEE Topical Conf. Wireless Sensors Sensor Netw. (WiSNet)*, Austin, TX, USA, Jan. 2016, pp. 23–25.